Photoluminescence from Er^{3+} ion and SnO_2 nanocrystal co-doped silica thin films

Xiaowei Zhang (张晓伟)[1], Tao Lin (林 涛)[1], Xiaofan Jiang (江小帆)[1] Jun Xu (徐 骏)[1,2*], Jianfeng Liu (刘建峰)[1,2], Ling Xu (徐 岭)[1], and Kunji Chen (陈坤基)[1]

[1]*School of Electronic Science and Engineering, School of Physics, Nanjing University, Nanjing 210093, China*

[2]*Joint Research Centers Online of Solid State Microstructure, Network and Information Center, Nanjing 210093, China*

[*]*Corresponding author: junxu@nju.edu.cn*

Received April 19, 2012; accepted April 25, 2012; posted online July 13, 2012

Er^{3+} ions embedded in silica thin films co-doped by SnO_2 nanocrystals are fabricated by sol-gel and spin coating methods. Uniformly distributed 4-nm SnO_2 nanocrystals are fabricated, and the nanocrystals showed tetragonal rutile crystalline structures confirmed by transmission electron microscope and X-ray diffraction measurements. A strong characteristic emission located at 1.54 μm from the Er^{3+} ions is identified, and the influences of Sn doping concentrations on photoluminescence properties are systematically evaluated. The emission at 1.54 μm from Er^{3+} ions is enhanced by more than three orders of magnitude, which can be attributed to the effective energy transfer from the defect states of SnO_2 nanocrystals to nearby Er^{3+} ions, as revealed by the selective excitation experiments.

OCIS codes: 160.4236, 160.5690, 160.2160, 260.3800.

doi: 10.3788/COL201210.091603.

There has been a growing interest in strong luminescence from rare-earth (RE) ions in the silica matrix because of their practical applications in high-brightness displays and optical communications[1−4]. However, the optical cross-sections of RE ions are usually rather small, resulting in low emission efficiency. This problem may be remedied by introducing semiconductor nanocrystals into the RE ion-doped silica thin films. Co-doping of semiconductor nanocrystals with europium (Eu) ions in silica thin films has been found to enhance significantly the characteristic emission at 614 nm[5−8]. The detailed excitation and luminescence process are still not fully understood, although the energy transfer mechanism has been proposed to explain the enhanced luminescence[9]. The co-doped nanocrystals are believed to act as sensitizers (donor) in a host matrix to enhance the luminescence from Eu^{3+} ions (activator) by non-radiative energy transfer process.

The characteristic emission at 1.54 μm from erbium (Er) ions is very important, especially in Si-based photonics[10]. The energy transfer from semiconductor nanocrystals to Er^{3+} ions, by co-doping the semiconductor nanocrystals, can efficiently compensate the small cross-section of transitions of Er^{3+} ions, typically in the order of 10^{-21} cm^{-2}[11,12]. In this letter, we use sol-gel and spin coating technique to prepare silica thin film co-doped by SnO_2 nanocrystals and Er^{3+} ions. SnO_2 nanocrystals can act as sensitizers in silica films, and their wide band gap (approximately 3.6 eV) can prevent the back energy transfer process efficiently[13−15]. Moreover, SnO_2 nanocrystals can be easily prepared in a controllable manner during sol-gel fabrication process, and their thermal stability is better than those of In_2O_3[8,16] and ZnO[17] nanocrystals. Results from transmission electron microscopy and X-ray diffraction show that the prepared SnO_2 nanocrystals have the average size of 4 nm and exhibit tetragonal rutile structures. The emission of 1.54 μm from Er^{3+} ions can be observed at room temperature from Er^{3+} ion and SnO_2 nanocrystal co-doped silica thin films. The influence of SnO_2 nanocrystal co-doping on the emission from Er^{3+} ions is investigated, and the luminescence intensity is obviously enhanced with SnO_2 nanocrystal co-doping. The mechanism of luminescence enhancement is discussed based on photoluminescence (PL) and photoluminescence excitation (PLE) spectra.

Silica, Er^{3+} ions, and SnO_2 nanocrystals were selected as the host material, activator ions, and embedded sensitizers, respectively. Tetraethyl orthosilicate, $SnCl_4$, and $Er(NO_3)_3$ were dissolved in a mixture of ethanol and deionized water with a molar ratio of 4:1 under rigorous stirring. After total dissolution, HCl was used as catalyst and dropped into the mixture to adjust the pH value to 2.0. Then, the precursor solution was refluxed at 60 °C for 4 h to complete hydrolysis. With these precursors, the spin coating method was used to prepare thin films on single polished silicon substrates. Spin coating was performed at 5 500 rpm. After spin coating, the prepared films were pyrolyzed at 450 °C in air for 30 min. The obtained films were annealed at 1 000 °C for 4 h at a ramp rate of approximately 6 °C/min under air ambient. In the above process, the concentration of Er^{3+} ions added into the precursor solution was fixed at 3 mol%, whereas the concentration of Sn was changed from 0 to 30 mol%. We used these values to label the final samples with different Sn or Er doping concentrations.

The microstructures of the thin film were investigated by a field emission transmission electron microscope (TEM) (TECNAI-F20). Film thickness of the different samples, ranging from 105 to 139 nm, was determined by an ellipsometer. In addition, the aged gel was dried at 60 °C, milled into fine powder, and then calcined at 1 000 °C for X-ray diffraction (XRD), with 0.15418-nm CuKα radiation. PL and PLE spectra were obtained using a spectrometer (Jobin Yvon Fluorolog-3) equipped with a 325-nm He-Cd laser and a 450-W Xe lamp as

the light sources. The spectra were corrected by the instrumental response. A long wavelength-enhanced InGaAs PIN photodiode with lock-in technology and a photomultiplier (Hamamatsu 928 PMT) were used as detectors during the PL and PLE tests.

The TEM images of a sol-gel silica film are presented to investigate the microstructures of the Sn and Er^{3+} ion co-doped thin film. The cross-sectional TEM image of the sample is shown in Fig. 1(a). The film thickness is approximately 110 nm, consistent with that measured using an ellipsometer. The film surface is quite smooth, indicating good-quality film. A high resolution TEM image of the 20 mol% Sn and 3 mol% Er co-doped silica thin film after annealing at 1 000 °C is shown in Fig. 1(b). The average size of the nanocrystals is approximately 4 nm, and the interplanar distance is 0.338 nm, corresponding to the (110) lattice spacing of the SnO_2 tetragonal phase. The uniform size distribution of the SnO_2 nanoparticles with an average size of approximately 4 nm is demonstrated in Fig. 1(c).

The XRD pattern for the corresponding sol-gel SiO_2 powder samples containing 20 mol% Sn and 3 mol% Er after annealing at 1 000 °C is demonstrated in Fig. 2 to characterize further the formation of SnO_2 nanoparticles. The pattern shows all the diffraction peaks assigned to the tetragonal rutile crystalline phase of the SnO_2 crystal (JCPDS No. 41-1445), consistent with the TEM results. No other phase of SnO_2 crystal is found after annealing at 1 000 °C, indicating that the SnO_2 nanocrystals with tetragonal rutile crystalline phase are more stable than those with other structures under our preparation conditions.

PLE and PL spectra of the Er^{3+} ion-free samples co-doped with 20 mol% Sn in silica host matrix after annealing at 1 000 °C are depicted in Fig. 3. Both PLE

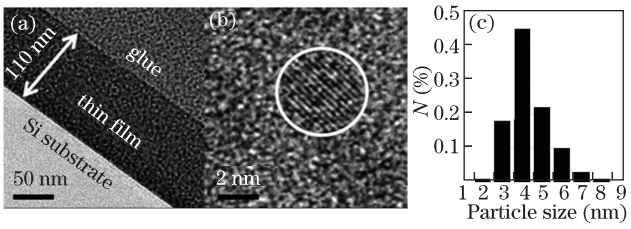

Fig. 1. (a) Cross-sectional TEM image of the 20 mol% Sn and 3 mol% Er co-doped silica thin film, (b) high resolution TEM image of the same thin film, and (c) size distribution of SnO_2 nanoparticles.

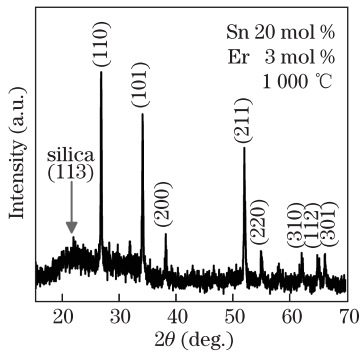

Fig. 2. XRD patterns of the 20 mol% Sn and 3 mol% Er co-doped SiO_2 powder samples after annealing at 1 000 °C.

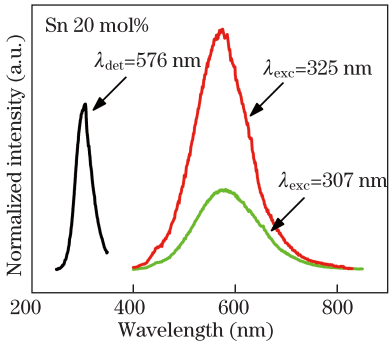

Fig. 3. PL spectra of Er^{3+}-free thin film annealed at 1 000 °C under the excitation wavelength of 325 nm from the laser and 307 nm from the Xe lamp on the right side, and PLE spectra of the same samples by detecting emission at 576 nm on the left side.

and PL signals are corrected by subtracting the spectral background. For PL measurements, the peak center located at 576 nm is observed using the 325-nm He-Cd laser as an excitation light source. No emission peak is detected under the same experimental conditions for the thin film without SnO_2 nanocrystals.

The PLE spectra are measured by keeping the detected wavelength at the peak center of 576 nm to confirm further the origin of the emission peak. A sharp excitation band with a maximum at approximately 307 nm is observed, indicating that the SnO_2 nanocrystals have a band gap of 4.04 eV. The band gap is larger than that of the SnO_2 bulk counterpart, and can be explained experimentally as the quantum confinement effect. With an Xe lamp as the excitation light, the excitation wavelength is maintained at 307 nm, and a wide band ranging from 400 to 800 nm is observed. The emission band is ascribed to the SnO_2 nanocrystals. Based on previous reports[18–20], the emission band originates from the defect states on the surface of the SnO_2 nanocrystals, such as the oxygen vacancies, tin interstitials, or dangling on the SnO_2 nanocrystal surface. Moreover, the wide emission band overlaps with the excitation spectra of Er^{3+} ions, attributable to the possible energy transfer.

We investigated the PL changes for co-doped samples with Sn concentrations varying from 0 to 30 mol% with constant Er^{3+} ion concentration at 3 mol%. As shown in Fig. 4, the film without Sn doping shows a weak peak at 1.54 μm. This characteristic emission is ascribed to the $^4I_{13/2}-^4I_{15/2}$ transition of the Er^{3+} ions. The luminescent intensity of the Er^{3+} ions at 1.54 μm is enhanced by more than three orders of magnitude at 20 mol% Sn concentration. The energy transfer process is effective because of the formation of SnO_2 nanocrystals with suitable size and density in the silica matrix after 1 000 °C annealing[14]. Moreover, as shown in the PL spectra, increasing Sn concentration is an effective way to enhance luminescence. The average distance and the total area of interface between the SnO_2 nanoparticles and Er^{3+} ions play important roles in the energy transfer process. The PL intensity increases monotonously with increasing Sn concentration from 0 to 20 mol%, attributable to more SnO_2 nanocrystals involved in the energy transfer process. With increasing Sn concentration, the total area of the interface between the SnO_2 nanoparticles and

Er^{3+} ions gradually increases, and the average distance between the SnO_2 nanoparticles and Er^{3+} ions gradually decreases. This phenomenon leads to higher energy transfer efficiency. However, superfluous Sn will lead to luminescent saturation and quenching when the concentration of Sn is more than 20 mol%. This condition may be explained by the fact that excessive Sn concentration leads to the agglomeration of nanocrystals and decrease in surface-to-volume ratio because of the increased particle size, which influences PL intensity[16].

To understand further the energy transfer process, PLE spectra of co-doped silica thin films are examined by keeping the detected emission wavelength at 1.54 μm, corresponding to the characteristic emission of the Er^{3+} ions. The PLE results are presented in Fig. 5. From the PLE spectra of the thin film with 0 mol% Sn and 3 mol% Er, several sharp excitation peaks can be found. The peaks located at 382 and 527 nm can be clearly identified. The resonant excitation located at 382 nm is related to the Er^{3+} ion transition from $^4I_{15/2}$ to $^4F_{5/2}$, whereas the one located at 527 nm results from the transition from $^4I_{15/2}$ to $^4S_{3/2}$[21,22]. For comparison, the PLE spectra from the thin sample co-doped 20 mol% Sn and 3 mol% Er are detected. Interestingly, in addition to the sharp excitation peaks from the 4f-4f transitions of the Er^{3+} ions, there are two wider and stronger excitation bands located at 307 and 576 nm. The two excitation bands can be attributed to the band gap and the defect states from the SnO_2 nanocrystals, respectively. Based on these measured results, we infer two possible channels for the excitations of the Er^{3+} ions. The several sharp excitation peaks indicate a direct excitation of the Er^{3+} ions from the ground state to the excited one, whereas the wide excitation bands indicate an indirect excitation by an energy transfer from the band gap and the defect states of the SnO_2 nanocrystals to Er^{3+} ions[15]. These conditions explain why the characteristic emission of the Er^{3+} ions, located at 1.54 μm, is enhanced by adding the SnO_2 nanocrystals.

The enhanced Er^{3+} ion emission can be attributed to the energy transfer process between the SnO_2 nanocrystals and Er^{3+} ions in co-doped films. SnO_2 nanocrystals are apparently pumped by incident photons and generate electron and hole pairs. The photo-excited electrons are then trapped by the defect states through non-radiative

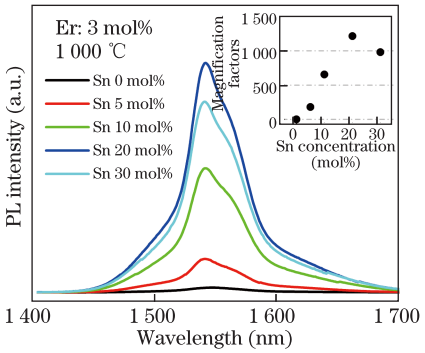

Fig. 4. PL spectra of thin films with 3 mol% Er^{3+} ions co-doped with different concentrations of Sn (0 to 30 mol%) under the excitation wavelength of 325 nm. Inset shows the changes in the characteristic emission intensity of Er^{3+} ions at 1.54 μm as a function of the Sn concentration.

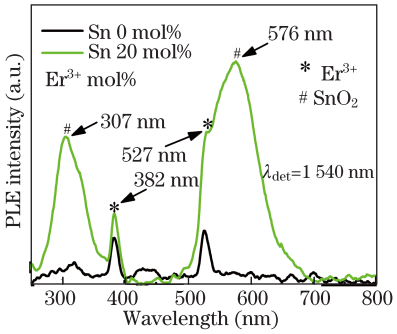

Fig. 5. PLE spectra of thin films with 3-mol% Er^{3+} ions co-doped with different concentrations of Sn (0 or 20 mol%) by detecting emission wavelength at 1.54 μm.

decay process. Considering the matching of SnO_2 defect state energy levels and the excitation energy of Er^{3+} ions, the Förster energy transfer can occur between the SnO_2 nanocrystals and the nearby Er^{3+} ions. This phenomenon causes the electron jump from the ground state to the excited ones in Er^{3+} ions and generates the Er^{3+} ions' characteristic emissions through the subsequent radiative relaxations. These processes are dominated by spectral overlapping, density of SnO_2 nanocrystals, and surrounding environment of Er^{3+} ions. SnO_2 nanoparticle is a good and inherent energy donor to Er^{3+} ions because of the good spectral overlapping.

According to the Fermi's "golden rule", the energy transfer probability is governed by the space distance between the donor and acceptor[17]. In this case, Er^{3+} ions occupy the silica matrix, and the most effective energy transfer occurs between SnO_2 nanocrystals and the nearest Er^{3+} ions. With increasing Sn concentrations, SnO_2 nanocrystals can be formed and grown to suitable size and density. Thus, the energy transfer is efficient and luminescence can be enhanced, as seen in our experimental results.

In conclusion, SnO_2 nanocrystal and Er^{3+} ion co-doped silica thin films are prepared by sol-gel process and spin coating method. The obtained SnO_2 nanocrystals are uniformly distributed, with size of approximately 4 nm. The influence of the concentration of Sn on the characteristic emission of the Er^{3+} ions at 1.54 μm is systematically investigated. Compared with the Sn-free samples, the emission at 1.54 μm could be enhanced by more than three orders of magnitude when the concentration of Sn is 20 mol%. Our experimental results indicate that the UV incident photons are absorbed by SnO_2 nanocrystals through band-to-band and band-to-defect state transitions, whereas the energy transfer process is from the defect states of SnO_2 nanocrystals to the nearby Er^{3+} ions. Moreover, further increasing the Sn concentration above 20 mol% induces the aggregation of large-sized SnO_2 nanocrystals, resulting in the increase of the average distance between Er^{3+} ions and SnO_2 nanocrystals. As a consequence, the luminescence becomes weaker because of the reduced energy transfer probability.

This work was supported by the Natural Science Foundation of Jiangsu Province (No. BK2010010), the "333" Project, and the Fundamental Research Funds for the Central Universities (Nos. 1112021001 and 1116021003).

References

1. M. J. Weber, J. Non-Cryst. Solids. **123,** 208 (1990).
2. W. Chen, J. O. Bovin, A. G. Joly, S. P. Wang, F. H. Su, and G. H. Li, Phys. Chem. B **108,** 11927 (2004).
3. A. Najar, J. Charrier, N. Lorrain, and L. Haji, Appl. Phys. Lett. **91,** 121120 (2007).
4. J. Vela, B. S. Prall, P. Rastogi, D. J. Werder, J. L. Cassion, D. J. Williams, V. I. Klimov, and J. A. Hollingsworth, J. Phys. Chem. C **112,** 20246 (2008).
5. G. Jose, G. Jose, V. Thomas, C. Joseph, M. A. Ittyachen, and N. V. Unnikrishnan, Mater. Lett. **57,** 1051 (2003).
6. I. Atsushi and K. Yoshihiko, Appl. Phys. Lett. **86,** 253106 (2005).
7. C. C. Lin, K. M. Lin, and Y. Y. Li, J. Luminescence **126,** 795 (2007).
8. N. Wan, J. Xu, T. Lin, X. G. Zhang, and L. Xu, Appl. Phys. Lett. **92,** 2011109 (2008).
9. N. Wan, T. Lin, J. Xu, L. Xu, and K. J. Chen, Nanotechnology **19,** 095709 (2008).
10. M. Fujii, M. Yoshida, Y. Kanzawa, S. Hayashi, and K. Yamamoto, Appl. Phys. Lett. **71,** 1198 (1997).
11. L. Eldada, Rev. Sci. Instrum. **75,** 575 (2004).
12. D. J. Lockwood and L. Pavesi, Top. Appl. Phys. **94,** 1 (2004).
13. Y. L. Yu, D. Q. Chen, P. Huang, H. Lin, A. P. Yang, and Y. S. Wang, J. Solid State Chem. **184,** 236 (2011).
14. M. Nogami, T. Enomoto, and T. Hayakawa, J. Luminescence **97,** 147 (2002).
15. S. Brovelli, A. Chiodini, A. Lauria, F. Meinardi, and A. Paleari, Phy. Rev. B **73,** 073406 (2006).
16. T. Lin, X. Y. Ding, J. Xu, N. Wan, L. Xu, and K. J. Chen, J. Appl. Phys. **109,** 083512 (2011).
17. J. Bang, H. Yang, and P. H. Holloway, J. Chem. Phys. **123,** 084709 (2005).
18. T. Lin, N. Wan, J. Xu, L. Xu, and K. J. Chen, J. Nanoscience and Nanotechnology **10,** 4357 (2010).
19. F. Gu, S. F. Wang, and C. F. Song, Chem. Phys. Lett. **372,** 451 (2003).
20. F. Gu, S. F. Wang, M. K. Lu, X. F. Cheng, S. W. Liu, G. J. Zhou, D. Xu, and D. R. Yuan, J. Crystal Growth **262,** 182 (2004).
21. X. T. Zhang, Y. C. Liu, J. G. Ma, Y. M. Lu, D. Z. Shen, W. Xu, G. Z. Zhong, and X. W. Fan, Thin Solid Films **413,** 257 (2002).
22. X. Zhao, S. Komuro, H. Isshiki, Y. Aoyagi, and T. Sugano, J. Luminescence **87,** 1254 (2000).